Quality Improvement Study

Medicine®

OPEN

Application of siemens SMART neuro attenuation correction in brain PET imaging

Xiaonan Shao, MD, Mei Xu, MD, Chun Qiu, MD, Rong Niu, MD, Yuetao Wang, MD, Xiaosong Wang, MD*

Abstract

Siemens SMART neuro attenuation correction (SNAC) is a new type of calculated attenuation correction (CAC) method. This article aimed to evaluate the effect of SNAC on the quantitative analysis of brain positron emission tomography (PET) imaging.

Brain PET images of 52 healthy participants after reconstructed by SNAC and CT attenuation correction (CTAC) were analyzed qualitatively by visual analysis, and quantitatively by Scenium software to compare their contrast, signal-to-noise ratio (SNR) as well as the mean standardized uptake value (SUV_{mean}) of different brain regions.

Compared with CTAC, reconstruction of images by SNAC significantly reduced the SNR by 17.3% ($P < .001$), but not affected the contrast ($P = .440$). In addition, the SUV_{mean} of different brain regions in images reconstructed by SNAC is increased, but still significantly correlated with that by CTAC ($r = 0.988$, $P < .001$), with a coefficient of $R^2 = 0.976$ in linear regression analysis. Moreover, the mean percent difference of SUV_{mean} between images reconstructed with SNAC and CTAC was 8.03% ± 5.38%, varying significantly in the range of −7.56% to 75.31% among 10 different brain regions ($F = 35.702$, $P < .001$) and showed greater percent difference in the peripheral brain regions than in the mesial brain regions.

Image reconstruction by SNAC has greater effect on quantitative analysis by increasing SUV_{mean} of different brain regions to varying degrees, but has little influence on the brain PET image quality. Moreover, it simplifies examination process and reduces radiation dose, which is beneficial to pediatric patients as well as serial scans to monitor therapy.

Abbreviations: CAC = calculated attenuation correction, CT = computed tomography, CTAC = CT attenuation correction, MNI = Montreal Neurological Institute, PET = positron emission tomography, ROI = region of interest, SNAC = Siemens SMART neuro attenuation correction, SNR = signal-to-noise ratio, SUV_{mean} = the mean standardized uptake value.

Keywords: attenuation correction methods, image processing, positron emission tomography, quality control

1. Introduction

In recent years, application of brain positron emission tomography (PET) imaging is increasing in the field of brain science research, including brain tumor diagnosis,[1] Alzheimer disease' diagnosis,[2] and cognitive function research.[3] It has been believed for a long time that photon attenuation in tissues is the most important physical factor affecting image quality and quantitative accuracy. Thus, quantitative PET image reconstruction requires an accurate attenuation map to compensate for attenuation.

Currently, the most commonly used methods for image attenuation correction include the calculated (transmissionless) methods and the measured (transmission-based) methods.[4] It is reported that compared with the calculated methods, the measured methods have the smallest bias and are more accurate in absolute quantification. Thus, they are considered as the "criterion standard" in 3D brain PET imaging.[4,5] The computed tomography (CT) transmission scan provides not only accurate anatomical localization information, but highly accurate attenuation correction data for PET imaging; thus, CT attenuation correction (CTAC) is widely used.[6] Quinn et al[7] recently found that in PET/CT examination, the brain is the third organ only to the bladder and heart with highest organ equivalent doses. The average organ equivalent dose of brain is 5.3 to 6.0 mGy from the standard registration CT, 16.1 to 21.0 mGy from the diagnostic quality CT and 15.9 to 17.3 mGy from ^{18}F-FDG.[7] Thus, radiation in CTAC cannot be ignored. In addition, the increased awareness of the exposure risk of ionizing radiation has also prompted us to minimize the radiation dose of nuclear medicine imaging.[8]

The development of approximation method is promoted by the uniformity of the tissues in head area to reduce the radiation dose. Calculated attenuation correction (CAC) was first proposed by Huang et al[9,10] and has undergone manual contour delineation, automatic edge detection algorithms,[11] and more refined algorithms to compute a 3-component attenuation map for brain PET imaging.[12] However, invalid assumption of tissue uniformity may lead to significant bias in activity quantification, especially in regions with high variability, such as air cavities and nasal sinuses. Template or atlas-guided attenuation correction[13] has overcome the problem by inferring anatomy from a head atlas, but there are still patient-specific problems.

Previous studies have shown that among various attenuation correction methods, CAC has the largest bias from the "criterion standard".[5] SMART neuro attenuation correction (SNAC) is a new type of CAC proposed in 2015 and can be used in the absence

Editor: Michael Masoomi.

XS and MX are co-first authors.

The authors report no conflicts of interest.

Department of Nuclear Medicine, the third affiliated hospital of Soochow University, Changzhou, China.

* Correspondence: Xiaosong Wang, Department of Nuclear Medicine, The Third Affiliated Hospital of Soochow University, Changzhou 213003, China (e-mail: wxs1732@163.com).

Medicine (2018) 97:38(e12502)

Received: 24 October 2017 / Accepted: 30 August 2018

http://dx.doi.org/10.1097/MD.0000000000012502

of anatomical information to model tissue and bone structures using the attenuation and scatter uncorrected PET data within the attenuation map.[14] The method is similar to the automatic contour detection method for attenuation map modeling as described by Bergstrom et al.[11] However, SNAC is performed by identifying the contours in the image domain instead of the sinogram domain. In this study, visual analysis and Scenium software were used to compare brain PET images reconstructed by SNAC and CTAC and to evaluate the effect of SNAC on qualitative and quantitative analyses of brain PET images.

2. Materials and methods

2.1. General information

The study was approved by the Ethics Committee of our institute. All patients and their family members signed the informed consent form. Patients' medical records were anonymous. From September 2016 to June 2017, a total of 30 male and 22 female healthy volunteers aged 36 to 82 years' old underwent whole-body PET/CT imaging at the Third Affiliated Hospital of Soochow University, Jiangsu Province, China. They all had blood glucose in the range of 4.5 to 5.9 mmol/L and met the following inclusion criteria: previously healthy and recently no discomfort; no abnormal brain mass, brain malformation, cerebrovascular diseases, as well as major organ diseases in other parts of the body such as malignant tumors found in PET/CT examination; fasting blood-glucose <6.0 mmol/L before PET examination; no history of cerebrovascular accidents, epilepsy, brain trauma, brain tumor; mental abnormalities, alcohol or drug abuses, as well as metabolic disorders such as hyperthyroidism and diabetes; and right preference.

2.2. Imaging method

The German Siemens Biograph mCT (64) type PET/CT device was used for imaging (Siemens Medical Solutions, Hoffman Estates, IL). Fluorine-18 fluorodeoxyglucose (^{18}F-FDG) of radiochemical purity >95% was supplied by the AMS Ltd (Nanjing, Jiangsu Province, China). The procedure of PET/CT imaging for ^{18}F-FDG metabolic mapping was as follows: the examinee began fasting at 20:00 of the day before the examination, and had an adequate sleep; blood glucose, body height, and body weight were measured before injection; ^{18}F-FDG was injected intravenously according to the dosage of 5.55 MBq/kg of body weight, after which a quiet rest for 30 minutes was requested; the topogram positioning scan was performed with tube current of 25 mA, voltage of 80 kV, scanning thickness of 0.6 mm, scan time of 2.7 s, and CT dose of 0.03 mGy; scanning range (1 PET bed) was selected and a diagnostic CT scan was performed with tube current of 370 mAs, voltage of 100 kV, collimation of 64x0.6 mm, pitch factor of 0.7, scan time of 18.36 seconds, CT dose of 36.35 mGy, and reconstruction thickness of 3.0 mm; and the PET scan was performed for 5 minutes per bed.

The CT-based attenuation map was obtained from the reconstructed CT slices by applying appropriate conversion factors and interpolating to match the reconstructed PET resolution. The image matrices of the PET image reconstruction algorithms were 512 with an amplification of 2.5 and Gaussian filtering with full width at half maximum of 1.5 mm. TrueX + TOF[15] method was applied with 6 iterations and 21 subsets.

The SNAC method uses the simple, uniform geometry and tissue distribution of the brain to visualize tissue/air boundaries from nonattenuation corrected PET scans to simulate attenuation maps. The contour is dilated by 4 mm to prevent artifacts at the edges. Once the perimeter of the brain was measured, a 4-mm thick bone tissue was imaged at 4 mm from the boundary, and the assigned attenuation values were divided into 3 levels: air = 0.000/cm, soft tissue = 0.093/cm, and bone = 0.140/cm. Figure 1B shows an axial view of the SNAC attenuation map obtained for a patient study. The reconstruction parameters for PET image reconstruction with SNAC were identical to those used with CTAC.

2.3. Image analysis and processing

Two experienced nuclear medicine physicians were responsible for the visual comparison of the brain PET images obtained by the 2 reconstruction methods. These reconstructed PET images were registered to the standard Montreal Neurological Institute (MNI) anatomical template.[16] Once registered to the MNI space, the mean standardized uptake value (SUV_{mean}) was calculated for 10 basic brain regions including the frontal lobe, temporal lobe, parietal lobe, cingulate and paracingulate gyri, central region, occipital lobe, calcarine fissure and surrounding cortex, basal ganglia, mesial temporal lobe, and cerebellum by Siemens brain function analysis software (Scenium). According to Nagaki et al,[17] the contrast was calculated using the following formula:

$$\text{Contrast} = \frac{C_{max} - C_{min}}{C_{min}} \quad (1)$$

wherein C_{max} and C_{min} are the maximum and minimum SUV_{mean} of different brain regions, respectively. The signal-to-noise ratio (SNR) was defined as the uniformity of the region of interest (ROI) of inside the cerebellum and calculated as

$$\text{SNR} = \frac{\text{Mean}}{SD} \quad (2)$$

wherein mean and SD represent the mean and standard deviation of the cerebellar with diameter of 1.1 cm within the ROI.

According to Li et al.,[18] the relative error of SUV_{mean} values of the 2 reconstruction methods were calculated as

$$\text{Percent difference} = \frac{SUV_{snac} - SUV_{ctac}}{SUV_{ctac}} \times 100\% \quad (3)$$

2.4. Statistical analysis

Statistical analysis was performed using the statistical package for the social scientists (SPSS version 13, Chicago, IL). Measurement data were denoted by $\overline{x} \pm s$. Two sets of data were compared using the t test and multiple sets of data were compared using 1-way analysis of variance. Intraset pairwise comparisons were performed using the Student-Newman-Keuls test. The paired SUV_{mean} data sets were compared using a paired t test. The correlation of SUV_{mean} of the 2 reconstruction methods was analyzed by Pearson correlation analysis and linear regression analysis.[19] P value <.05 was considered statistically significant.

3. Results

3.1. Qualitative analysis

Brain PET images reconstructed using CTAC and SNAC methods (Fig. 1C and D) were compared through visual comparison by 2 experienced nuclear medicine physicians and no significant difference in image quality was found.

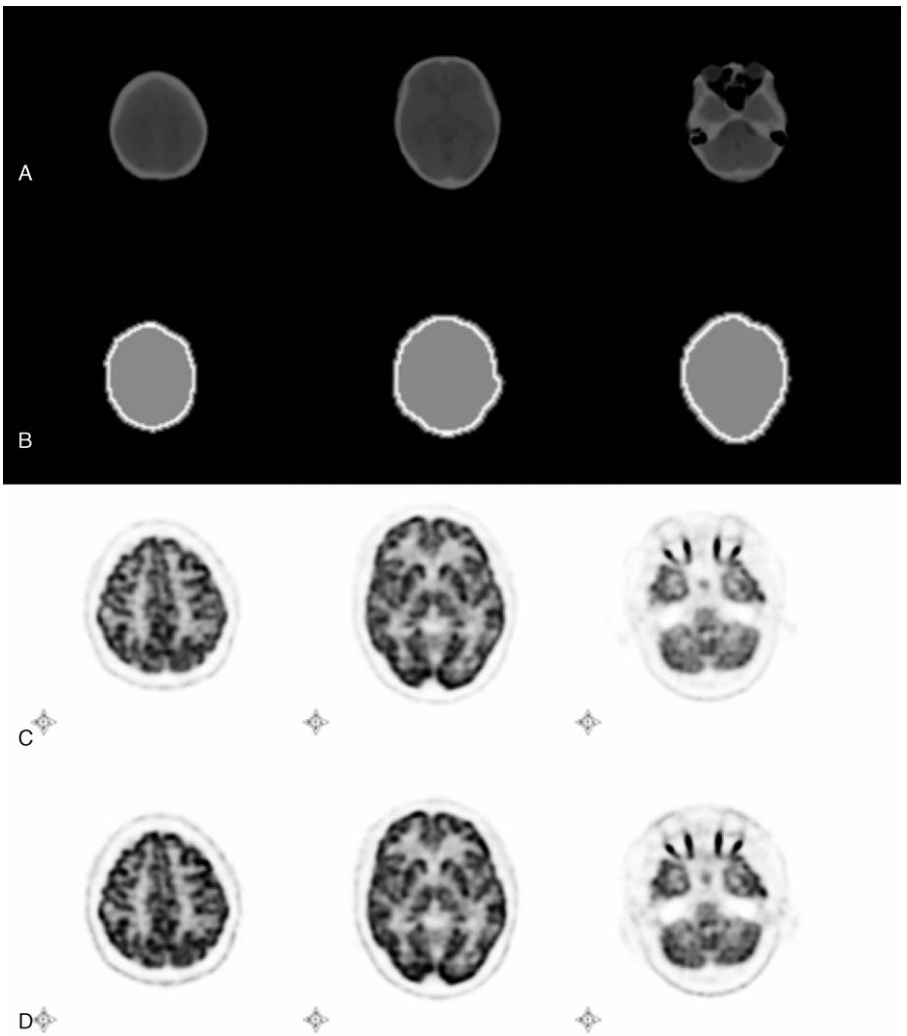

Figure 1. Axial view of attenuation map obtained with CT attenuation correction (CTAC) (A) and Siemens SMART neuro attenuation correction (SNAC) (B) as well as PET images reconstructed with CTAC (C) and SNAC (D) ($T=18.0$, B=0, slice thickness=1.5 mm).

3.2. Quantitative analysis

CTAC and SNAC images were analyzed using Scenium software. The results of analyses of variance showed that SUV_{mean} of different brain regions obtained by the 2 methods were significantly different ($F=19.443$ and 18.711, all $P<.01$), showing the maximum in the calcarine fissure and surrounding cortex and minimum in the mesial temporal lobe (Fig. 2).

The contrast and SNR of CTAC and SNAC were calculated and compared using the paired *t* test. The results showed that the mean values for contrast were 0.77 ± 0.18 and 0.78 ± 0.21, respectively, showing no significant difference ($t=0.778$, $P=.440$), whereas the mean values for SNR were 9.17 ± 2.02 and 7.58 ± 1.69, respectively, showing significant difference ($t=11.732$, $P<.001$). The SNR of SNAC decreased by 17.3% compared with that of CTAC.

The reconstructed PET images of 10 basic brain regions using both SNAC and CTAC methods were analyzed using paired *t* test. The results showed that SUV_{mean} of all brain regions in SNAC were significantly higher than those in CTAC ($t=8.068$–24.890, all $P<.001$) (Fig. 2).

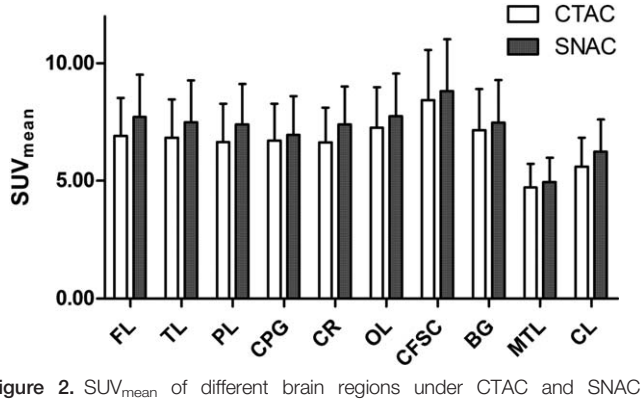

Figure 2. SUV_{mean} of different brain regions under CTAC and SNAC reconstruction methods. *x* Axis represents the different brain regions. BG=basal ganglia, CFSC=calcarine fissure and surrounding cortex, CL=cerebellum, CPG=cingulate and paracingulate gyri, CR=central region, CTAC=CT attenuation correction, FL=frontal lobe, MTL=mesial temporal lobe, OL=occipital lobe, PL=parietal lobe, SNAC=Siemens SMART neuro attenuation correction, SUV_{mean}=the mean standardized uptake value, TL=temporal lobe. *y* Axis represents SUV_{mean}.

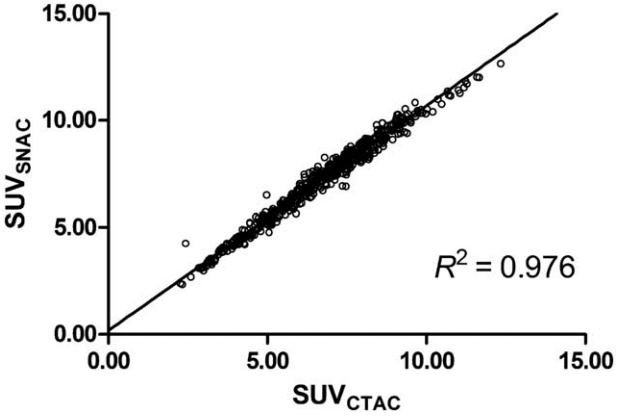

Figure 3. Correlations between SUV_{mean} of SNAC and CTAC. CTAC = CT attenuation correction, SNAC = Siemens SMART neuro attenuation correction, SUV_{mean} = the mean standardized uptake value.

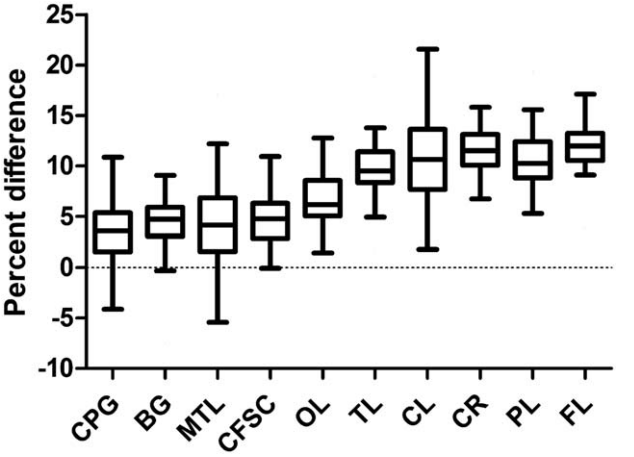

Figure 4. The percent differences in different brain regions under SNAC and CTAC reconstruction in an ascendant order. *x* Axis represents the different brain regions. *y* Axis represents percent differences. BG = basal ganglia, CFSC = calcarine fissure and surrounding cortex, CL = cerebellum, CPG = cingulate and paracingulate gyri, CR = central region, CTAC = CT attenuation correction, FL = frontal lobe, MTL = mesial temporal lobe, OL = occipital lobe, PL = parietal lobe, SNAC = Siemens SMART neuro attenuation correction, TL = temporal lobe

3.3. Correlation of SUVmean of the 2 reconstruction methods

The SUV_{mean} obtained using the 2 methods of a total of 520 brain regions of the 52 participants were used for Pearson correlation analysis. The result showed that SUV_{mean} obtained using the 2 methods had a significantly positive correlation ($r = 0.988$, $P < .001$). Their linear regression equation was $SUV_{SNAC} = 0.182 + 1.051SUV_{CTAC}$, $R^2 = 0.976$ (Fig. 3).

3.4. The relative difference of SUV_{mean} of the 2 reconstruction methods

The mean percent difference in SUV_{mean} of the 10 brain regions was $8.03\% \pm 5.38\%$ (-7.56% to 75.31%). The mean percent difference was the lowest of $3.61\% \pm 2.87\%$ in cingulate and paracingulate gyri region of the mesial brain regions and the highest of $11.84\% \pm 2.14\%$ in the frontal lobe of the peripheral brain regions; the brain regions with negative percent difference were cingulate and paracingulate gyri, calcarine fissure and surrounding cortex, basal ganglia, as well as mesial temporal lobe, all located in the mesial brain region (Fig. 4).

The results of analysis of variance showed that the percent difference of different brain regions between 2 reconstruction methods varied significantly ($F = 35.702$, $P < .001$). Then, further S-N-K tests were performed, and 10 brain regions were divided into 3 groups according to the mean percent difference and the statistical results. The mean percent differences in all regions within the group were not significantly different ($P > .05$). Comparison between the groups showed that the mean percent difference of the peripheral brain regions such as parietal lobe and frontal lobe was significantly greater than that of the mesial brain regions including cingulate and paracingulate gyri as well as basal ganglia ($P < .05$) (Table 1).

4. Discussion

Attenuation correction is an important step in qualitative and quantitative analysis of brain PET imaging. Theoretically, the attenuation correction method based on transmission scanning produces the smallest bias and is considered as the "criterion standard" of brain PET imaging.[4,5] CT is also a transmission scan. Since the advent of PET/CT, CTAC is widely used because it has advantages of rapidness, free from the subject's 511 keV γ photon interference, good data statistics, and low noise.[6] However, CTAC also has its limitations, such as increased radiation dose of subjects[20] and overestimation of SUV of high-density materials,[21,22] and may also result in image artifacts owing to patient motion between sequential scans.[23] In this study, we found that the visual image quality of SNAC and CTAC was not significantly different and application of both did not affect the subjective interpretation of PET images, in agreement with the results of Zaidi et al.[5] In addition, quantitative analysis showed that there was no significant difference in contrast, in line with the above results, although SNR of the SNAC method was lower.

Scenium software is an advanced neural evaluation tool based on ROI technology. It can automatically outline 10 basic brain regions according to the template and calculate the SUV_{mean}, thus avoiding the manual error. Therefore, it can be used for quantitative comparison of different brain imaging methods, and make the results more accurate and reliable.[15,24] Zaidi et al[5] found that CAC method had a large bias and could overestimate the metabolism of peripheral brain regions. In addition, its correlation with the "criterion standard" was not very good ($R^2 = 0.54$). In this study, although the SNAC increased the SUV_{mean} of different brain regions to a various degree, it was significantly correlated with CTAC results ($r = 0.988$), consistent with a recent research ($r = 0.98$) by Bal et al,[25] suggesting that the SNAC method is significantly improved compared with the traditional CAC.

The greatest limitation of CAC is the need to specify linear attenuation coefficients for different tissues, as does SNAC. Because of the presence of relatively low-density ventricular system in the brain, and CAC does not consider the attenuation coefficient of the sinus cavity and sinus cavity differences in different patients, which will lead to metabolic differences between the peripheral brain and mesial brain regions.[4,25] Zaidi et al[5] found that the relative difference of CAC's mean regional cerebral glucose metabolism was <8%. It has been shown that

Table 1

Percent difference comparison of SNAC and CTAC reconstruction methods in different brain regions.

Group	Brain region	Mean percent difference	P
Group I	Cingulate and paracingulate gyri	3.61 ± 2.87	.473
	Basal ganglia	4.28 ± 3.05	
	Mesial temporal lobe	4.60 ± 4.04	
	Calcarine fissure and surrounding cortex	4.82 ± 2.88	
Group II	Occipital lobe	6.78 ± 2.89	1.000
Group III	Temporal lobe	9.70 ± 2.68	.079
	Cerebellum	11.28 ± 5.04	
	Central region	11.56 ± 2.44	
	Parietal lobe	11.81 ± 9.35	
	Frontal lobe	11.84 ± 2.14	

CTAC = CT attenuation correction, SNAC = Siemens SMART neuro attenuation correction.

ignoring sinus air-like attenuation coefficient values can result in an overestimation of the tracer uptake by up to 20% in adjacent brain regions.[26] Bal et al[22] found that relative error for all regions was <5% for SNAC. For most of the regions, application of SNAC resulted in overestimation. The maximum absolute error for SNAC was observed in the right frontal lobe. In this study, the mean percent difference was 8.03% for SNAC images with respect to CTAC, which was larger in peripheral brain region than in the mesial brain region. These results indicated that the SNAC method overestimated the SUV_{mean} in the whole brain region, and that the SUV_{mean} in the peripheral brain region was overestimated more than that in the mesial brain region, thus significantly impacting the quantitative analysis. In theory, the difference between the peripheral and mesial regions of the brain could increase image contrast. Zaidi et al[5] also found by a relative quantitative approach that the contrast was superior in the images obtained using the CAC method than using the "criterion standard." But this improvement was not significant in this study.

Based on the importance of radiation dose, Xia et al[27] proposed that application of ultra-low-dose CT in PET/CT could reduce radiation dose. With the advent of PET/MRI, MRI data were widely applied for attenuation correction, but the skull will cause significant metabolic bias in different brain regions, affecting quantitative analysis.[28] Moreover, the coils of the MR may cause significant attenuation of the annihilation radiation leading to artefacts and biases in the reconstructed activity concentrations.[29] Lowering radiation dose is particularly desired in application for pediatric imaging as well as serial scans to monitor therapy.[30–32] In this study, because CT scan is for diagnose, the radiation dose of CT was 2 times higher than that of PET. In addition, SNAC uses an uncorrected PET map to create the attenuation map, which only takes 6 seconds, and thus improves image reconstruction speed. However, further work is required to assess the clinical advantage of SNAC.

Overall, SNAC is a robust method for FDG brain PET imaging. However, as a transmissionless attenuation correction method, it increases SUV_{mean} of different brain regions to varying degrees and has a greater impact on quantitative analysis. In the future, NEMA brain phantom will be used to compare the accuracy of 2 attenuation correction methods. SNAC simplifies the examination process, reduces the radiation dose, and has no significant effect on image quality. Therefore, application of SNAC only for qualitative diagnosis may benefit pediatric patients as well as serial scans to monitor therapy.

Author contributions

Data curation: Mei Xu, Chun Qiu, Rong Niu.
Formal analysis: Mei Xu, Chun Qiu, Rong Niu.
Software: Xiaonan Shao.
Writing – original draft: Xiaonan Shao.
Writing – review & editing: Yuetao Wang, Xiaosong Wang.

References

[1] Suchorska B, Tonn JC, Jansen NL. PET imaging for brain tumor diagnostics. Curr Opin Neurol 2014;27:683–8.
[2] Marcus C, Mena E, Subramaniam RM. Brain PET in the diagnosis of Alzheimer's disease. Clin Nucl Med 2014;39:e413–422. quiz e423–416.
[3] Roberts RO, Knopman DS, Cha RH, et al. Diabetes and elevated hemoglobin A1c levels are associated with brain hypometabolism but not amyloid accumulation. J Nucl Med 2014;55:759–64.
[4] Zaidi H, Montandon ML, Meikle S. Strategies for attenuation compensation in neurological PET studies. NeuroImage 2007;34: 518–41.
[5] Zaidi H, Montandon ML, Slosman DO. Attenuation compensation in cerebral 3D PET: effect of the attenuation map on absolute and relative quantitation. Eur J Nucl Med Mol Imag 2004;31:52–63.
[6] Kinahan PE, Hasegawa BH, Beyer T. X-ray-based attenuation correction for positron emission tomography/computed tomography scanners. Semin Nucl Med 2003;33:166–79.
[7] Quinn B, Dauer Z, Pandit-Taskar N, et al. Radiation dosimetry of 18F-FDG PET/CT: incorporating exam-specific parameters in dose estimates. BMC Med Imaging 2016;16:41.
[8] Brink JA, Amis ESJr. Image Wisely: a campaign to increase awareness about adult radiation protection. Radiology 2010;257:601–2.
[9] Huang SC, Hoffman EJ, Phelps ME, et al. Quantitation in positron emission computed tomography: 2. Effects of inaccurate attenuation correction. J Comp Assist Tomogr 1979;3:804–14.
[10] Huang SC, Carson RE, Phelps ME, et al. A boundary method for attenuation correction in positron computed tomography, Journal of nuclear medicine: official publication. Soc Nucl Med 1981;22:627–37.
[11] Bergstrom M, Litton J, Eriksson L, et al. Determination of object contour from projections for attenuation correction in cranial positron emission tomography. J Comput Assist Tomogr 1982;6:365–72.
[12] Weinzapfel BT, Hutchins GD. Automated PET attenuation correction model for functional brain imaging, Journal of nuclear medicine: official publication. Soc Nucl Med 2001;42:483–91.
[13] Stodilka RZ, Kemp BJ, Prato FS, et al. Scatter and attenuation correction for brain SPECT using attenuation distributions inferred from a head atlas. J Nucl Med 2000;41:1569–78.
[14] Peyrat JM, Joshi A, Mintun M, et al. An automatic method for the quantification of uptake with Florbetapir imaging. Soc Nucl Med 2012;53(suppl 1):
[15] Shao X, Shao X, Wang X, et al. Applications of both time of flight and point spread function in brain PET image reconstruction. Nucl Med Commun 2016;37:422–7.
[16] Li Y, Wang D, Zhang H, et al. Changes of brain connectivity in the primary motor cortex after subcortical stroke: a multimodal magnetic resonance imaging study. Medicine 2016;95:e2579.

[17] Nagaki A, Onoguchi M, Matsutomo N. Clinical validation of high-resolution image reconstruction algorithms in brain 18F-FDG-PET: effect of incorporating Gaussian filter, point spread function, and time-of-flight. Nucl Med Commun 2014;35:1224–32.
[18] Li Y, Wang Y, Zhang H, et al. The effect of acupuncture on the motor function and white matter microstructure in ischemic stroke patients. Evid Based Complement Alternat Med 2015;2015: 164792.
[19] Zhang H, Wu W, Xu L, et al. Analysis of efficient biometric index using heart rate variability for remote monitoring of obstructive sleep apnea. Neuropsychiatry 2017;7:788–95.
[20] Huang B, Law MW, Khong PL. Whole-body PET/CT scanning: estimation of radiation dose and cancer risk. Radiology 2009;251: 166–74.
[21] Kinahan PE, Townsend DW, Beyer T, et al. Attenuation correction for a combined 3D PET/CT scanner. Med Phys 1998;25:2046–53.
[22] Visvikis D, Costa DC, Croasdale I, et al. CT-based attenuation correction in the calculation of semi-quantitative indices of [18F]FDG uptake in PET. Eur J Nucl Med Mol Imag 2003;30:344–53.
[23] Sureshbabu W, Mawlawi O. PET/CT imaging artifacts. J Nucl Med Technol 2005;33:156–61. quiz 163–154.
[24] Salsano E, Marotta G, Manfredi V, et al. Brain fluorodeoxyglucose PET in adrenoleukodystrophy. Neurology 2014;83:981–9.
[25] Bal H, Panin VY, Platsch G, et al. Evaluation of MLACF based calculated attenuation brain PET imaging for FDG patient studies. Phys Med Biol 2017;62:2542–58.
[26] Catana C, van der Kouwe A, Benner T, et al. Toward implementing an MRI-based PET attenuation-correction method for neurologic studies on the MR-PET brain prototype. J Nucl Med 2010;51:1431–8.
[27] Xia T, Alessio AM, De Man B, et al. Ultra-low dose CT attenuation correction for PET/CT. Phys Med Biol 2012;57:309–28.
[28] Andersen FL, Ladefoged CN, Beyer T, et al. Combined PET/MR imaging in neurology: MR-based attenuation correction implies a strong spatial bias when ignoring bone. NeuroImage 2014;84:206–16.
[29] Lerche CW, Kaltsas T, Caldeira L, et al. PET attenuation correction for rigid MR Tx/Rx coils from (176)Lu background activity. Phys Med Biol 2018;63:035039.
[30] Nelles G, Jentzen W, Bockisch A, et al. Neural substrates of good and poor recovery after hemiplegic stroke: a serial PET study. J Neurol 2011;258:2168–75.
[31] Hipp SJ, Steffen-Smith EA, Patronas N, et al. Molecular imaging of pediatric brain tumors: comparison of tumor metabolism using (1)(8)F-FDG-PET and MRSI. J Neuro-oncol 2012;109:521–7.
[32] Shokouhi S, Claassen D, Kang H, et al. Longitudinal progression of cognitive decline correlates with changes in the spatial pattern of brain 18F-FDG PET. J Nucl Med 2013;54:1564–9.